Published in Earth and Planetary Science Letters 386, issues 3-4, 414-425, 2009
which should be used for any reference to this work

Boron, lithium and strontium isotopes as tracers of seawater–serpentinite interaction at Mid-Atlantic ridge, ODP Leg 209

Flurin Vils [a,*], Sonia Tonarini [b], Angelika Kalt [a], Hans-Michael Seitz [c]

[a] *Institut de Géologie et d'Hydrogéologie, Université de Neuchâtel, Rue Emile-Argand 11, CP 158, 2009 Neuchâtel, Switzerland*
[b] *Istituto Geoscienze Georisorse, C.N.R. Pisa, Italy*
[c] *J.W. Goethe-Universität, Frankfurt, Germany*

A B S T R A C T

Spinel harzburgites from ODP Leg 209 (Sites 1272A, 1274A) drilled at the Mid-Atlantic ridge between 14°N and 16°N are highly serpentinized (50–100%), but still preserve relics of primary phases (olivine≥ orthopyroxene>>clinopyroxene). We determined whole-rock B and Li isotope compositions in order to constrain the effect of serpentinization on δ^{11}B and δ^{7}Li. Our data indicate that during serpentinization Li is leached from the rock, while B is added. The samples from ODP Leg 209 show the heaviest δ^{11}B (+29.6 to +40.52‰) and lightest δ^{7}Li (−28.46 to +7.17‰) found so far in oceanic mantle. High ^{87}Sr/^{86}Sr ratios (0.708536 to 0.709130) indicate moderate water/rock ratios (3 to 273, on the average 39), in line with the high degree of serpentinization observed.

Applying the known fractionation factors for ^{11}B/^{10}B and ^{7}Li/^{6}Li between seawater and silicates, serpentinized peridotite in equilibrium with seawater at conditions corresponding to those of the studied drill holes (pH: 8.2; temperature: 200 °C) should have δ^{11}B of +21.52‰ and δ^{7}Li of +9.7‰. As the data from ODP Leg 209 are clearly not in line with this, we modelled a process of seawater–rock interaction where δ^{11}B and δ^{7}Li of seawater evolve during penetration into the oceanic plate. Assuming chemical equilibrium between fluid and a rock with δ^{11}B and δ^{7}Li of ODP Leg 209 samples, we obtain δ^{11}B and δ^{7}Li values of +50 to +60‰, −2 to +12‰, respectively, for the coexisting fluid. In the oceanic domain, no hydrothermal fluids with such high δ^{11}B have yet been found, but are predicted by theoretical calculations. Combining the calculated water/rock ratios with the δ^{7}Li and δ^{11}B evolution in the fluid, shows that modification of δ^{7}Li during serpentinization requires higher water/rock ratios than modification of δ^{11}B.

Extremely heavy δ^{11}B in serpentinized oceanic mantle can potentially be transported into subduction zones, as the B budget of the oceanic plate is dominated by serpentinites. Extremely light δ^{7}Li is unlikely to survive as the Li budget is dominated by the oceanic crust, even at small fractions.

Keywords: ODP Leg 209, Δ_{11}B, Δ_{7}Li, ^{87}Sr/^{86}Sr, serpentinized harzburgite, peridotite

1. Introduction

At mid-ocean ridges, new oceanic crust is formed, and mantle may be exhumed at the ocean floor (e.g. Cannat, 1993; Escartin et al., 2003; Michael et al., 2003). The oceanic plate cools continuously as it moves away from the ridge. Hydrothermal activity is thought to play a major role in this cooling process and may be responsible for the discrepancies between observed and modelled heat flow values (Stein and Stein, 1992; Stein and Stein, 1996). Interaction between seawater and the oceanic plate alters the latter as secondary hydrous minerals precipitate. At relatively low temperatures, the latter preferentially incorporate the light elements B and Li and fractionation of ^{11}B from ^{10}B and of ^{7}Li from ^{6}Li takes place. During its residence in the ocean, the plate can become highly enriched in secondary minerals, containing more Li and B than unaltered mantle or oceanic crust and distinctive isotopic compositions (e.g. Ryan and Langmuir, 1987; Chan et al., 1992; Ryan and Langmuir, 1993; Bouman et al., 2004; Elliott et al., 2004; Tomascak, 2004; Chan et al., 2002). Alteration is therefore an important parameter controlling the input of light elements and their isotopes into subduction zones (e.g. Elliott et al., 2004; Savov et al., 2005; Savov et al., 2007; Vils et al., 2008).

At temperatures<100 °C, basalts exposed on the seafloor usually take up seawater B and Li through formation of alteration phases such as clay minerals (e.g. Seyfried et al., 1984; Chan et al., 1992; Ishikawa and Nakamura, 1992; Palmer and Swihart, 1996). The isotope fractionation is in general such that the heavy isotopes (^{7}Li, ^{11}B) are partitioned into the fluid whereas the light isotopes (^{6}Li, ^{10}B) are preferentially retained in the rock (e.g. Palmer and Swihart, 1996; Tomascak et al., 2008). However, as the clay minerals equilibrate with a reservoir of heavy Li and B, they will acquire relatively high δ^{11}B and

* Corresponding author. Department of Earth Sciences, University of Bristol, Wills Memorial Building, Queen's Road, BRISTOL BS8 1RJ United Kingdom. Tel.: +44 117 954 52 47 (office); fax: +44 117 925 33 85.
E-mail addresses: flurin.vils@bristol.ac.uk (F. Vils), s.tonarini@igg.cnr.it (S. Tonarini), angelika.kalt@unine.ch (A. Kalt), h.m.seitz@em.uni-frankfurt.de (H.-M. Seitz).

δ^7Li values compared to the unaltered rock. This has been shown in studies on altered basalts from the ocean floor (Chan et al., 1992; Ishikawa and Nakamura, 1992; Ishikawa and Nakamura, 1993) and by experimental equilibration of clay minerals and clay-rich sediments with seawater (e.g. Palmer et al., 1987; You et al., 1995; Vigier et al., 2008).

At temperatures above the upper stability limit of clay minerals (ca. 200 °C), chlorite becomes the most important secondary hydrous mineral in basalts and serpentine in peridotite. Although these phyllosilicates can potentially accommodate Li and B in their structures, it has been documented in several instances that at elevated temperatures, Li and B are leached from basalt (e.g. Ishikawa and Nakamura, 1992; Chan et al., 1993; Seyfried et al., 1998). As the fractionation in both isotope systems decreases with increasing temperature (e.g. Chan et al., 1992; Chan et al., 1993; Palmer and Swihart, 1996; Tomascak, 2004; Vigier et al., 2008), it might be expected that hydrothermally altered basalts and peridotites have δ^{11}B and δ^7Li values between those of their low-temperature equivalents and seawater. However, neither the elemental partition coefficients nor the isotope fractionation is known for chlorite-seawater and serpentine-seawater.

An increasing dataset on oceanic peridotite that interacted with seawater at ridges or fracture zones shows that serpentine minerals and serpentinite are generally enriched in B during alteration (10–100 μg/g), whereas they can be enriched (up to 13.7 μg/g) or depleted (down to 0.1 μg/g) in Li (Thompson and Melson, 1970; Bonatti et al., 1984; Spivack and Edmond, 1987; Niu, 2004; Boschi et al., 2008; Vils et al., 2008) compared to the values for depleted mantle (B: 0.06 μg/g, Li: 0.7 μg/g; Salters and Stracke, 2004). Samples of serpentinized peridotites from the Atlantis Massif (Boschi et al., 2008) and from the Atlantic ocean (Spivack and Edmond, 1987; Simon et al., 2006) show heavy δ^{11}B compared to mantle peridotites (+7.0 to +25.3‰ versus −3‰; Hart et al., 1999), but the spread is large. In-situ Li and δ^7Li measurements on serpentine from the Southwest Indian Ridge showed a range in δ^7Li from +25.5 to −19.1‰ (Decitre et al., 2002).

In order to explain the range in concentration (and isotopic composition) often found in serpentinized peridotites at one single site and displayed by fluids emerging from hydrothermal vents, several authors have invoked the importance of fluid–rock ratio and fluid evolution (Decitre et al., 2002; McCaig et al., 2007; Boschi et al., 2008). In our previous work (Vils et al., 2008) on serpentinized peridotites from ODP Leg 209 (Sites 1272A and 1274A) we showed by in-situ measurement of B and Li concentrations in minerals and whole-rock samples that during serpentinization B is taken up from seawater while Li is lost. Here, we present δ^{11}B, δ^7Li and ^{87}Sr/^{86}Sr values and Li concentrations of 17 whole-rock samples from the same ODP Leg. We discuss the results against the background of theoretical and observed B and Li isotope fractionation during seawater–peridotite interaction and model the latter for our case.

2. ODP Leg 209

ODP Leg 209 was drilled at the Mid-Atlantic ridge (Fig. 1) north and south of the Fifteen–Twenty fracture zone (Bach et al., 2004; Kelemen et al., 2004; Kelemen et al., 2007). Samples presented in this study are serpentinized harzburgites from Site 1272A and Site 1274A. The primary geochemical features of the mantle rocks at the two sites are slightly different, which is reflected in the REE patterns of whole-rock samples (Godard et al., 2008), but at both sites the peridotites show high degrees of partial melting and melt extraction (Seyler et al., 2007; Godard et al., 2008; Suhr et al., 2008). The degree of serpentinization varies between 51 and 99%. The rocks of Site 1272A are generally serpentinized to a higher degree as those of Site 1274A, with a down-hole decrease of serpentinization in the former. For detailed sample descriptions, major and light element contents of minerals and B contents of whole-rock samples, we refer to our previous study (Vils et al., 2008). The samples are composed of primary phases (olivine, orthopyroxene and two generations of clinopyroxene), and serpentine (mostly lizardite; Pelletier, 2008). Sample OD 42 contains one cluster of magmatic olivine left over from a passing melt. Primary phases (ol, opx and cpx), except second-generation clinopyroxene, show low Li, Be and B concentrations (<1 μg/g). Serpentine minerals are the major carrier of B (up to 177 μg/g), and second-generation clinopyroxene is the major phase for Li (up to 5.4 μg/g). No clay minerals or low-temperature phases other than serpentine are reported in the studied samples, with the exception of chlorite in OD 42 and possibly iowaiite in OD 34.

3. Analytical methods

Prior to any chemical treatment external rims of samples were systematically removed. Dust was washed off in an ultrasonic bath in MilliQ water for 10 min. 2–3 cm thick slabs from the drilled samples were crushed to μm size in an agate micromill at the ETH Zurich (CH).

B isotope composition was determined using a VG Isomass 54E positive ion thermal ionization mass spectrometer at IGG-CNR in Pisa, following B extraction and purification procedures described by Tonarini et al. (2003). Samples (ca. 1–1.5 μg B) were loaded onto single outgases tantalum filaments together with a graphite layer. B isotopic compositions of the samples are reported in the conventional delta notation (δ^{11}B) as per mil deviation from accepted composition

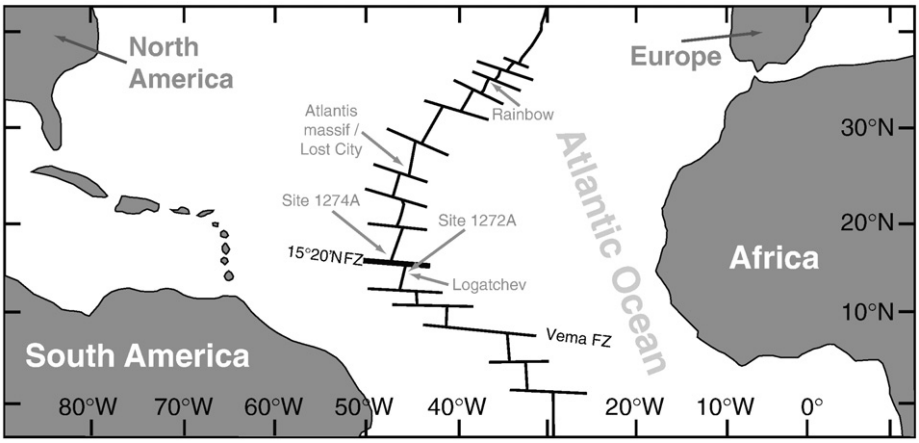

Fig. 1. Simplified map of the axial zone of the Mid-Atlantic Ridge, with situation of the ODP 209 drilling site north and south of the Fifteen–Twenty fracture zone (modified after Paulick et al., 2006). FZ, fracture zone.

of NIST-SRM 951 (certified $^{11}B/^{10}B = 4.04362$; Catanzaro et al., 1970). One analysis corresponds to 25–40 blocks of 10 individual B ratio measurements; in-run statistic is based on the block average. Accuracy of the procedure was evaluated by repeated analyses of NIST-SRM 951 standard taken through the full chemistry procedure (Supplementary Table 1). Isotopic fractionation associated with the mass spectrometer analysis was corrected using a fractionation factor calculated as $[(R_{cert} + 0.00079) / R_{meas}]$; $^{11}B/^{10}B_{meas}$ (NIST-SRM 951) = 4.0520 ± 0.0016 (2 SD). Replicate analyses of NIST-SRM 951 that did not undergo the chemical procedure gave $^{11}B/^{10}B_{meas}$ (SRM 951) = 4.0516 ± 0.0016 (2 SD, Supplementary Table 1). The reproducibility of analytical results for isotopically homogeneous samples treated with alkaline fusion chemistry is approximately ± 0.5‰. The analytical reproducibility for natural rock samples was estimated by replicate analyses of geological standard JB-2 ($^{11}B/^{10}B_{meas} = 4.0812 \pm 0.0018$ (2 SD, $N = 15$), corresponding to $\delta^{11}B$ of 7.50 ± 0.44 which is not statistically different from values of Nakamura et al. (1992) and Kasemann et al. (2001). The total procedural blank for the whole chemical treatment was 20 to 30 ng, thus negligible considering the processed boron aliquot.

Strontium isotope analyses were performed on a Finnigan MAT 262V multicollector mass spectrometer at IGG-CNR in Pisa, after conventional HF-HNO_3 dissolution and ion exchange procedures using Sr-SpecEIChroM resins for strontium separation from the matrix. Measured $^{87}Sr/^{86}Sr$ ratios were normalized to $^{86}Sr/^{88}Sr = 0.1194$. The quoted error on single measurement is the standard deviation of the mean ($2\sigma_{mean}$). During the collection of isotopic data, 6 replicate analyses of NIST-SRM 987 ($SrCO_3$) gave an average value of 0.710244 ± 12 (2 SD, Supplementary Table 1). All $^{87}Sr/^{86}Sr$ data were normalized to the certified value 0.71025 for the NIST-SRM 987 standard. Two total procedural blanks measured during sample analysis were 0.15 ng, negligible for analyzed samples.

Rock digestion and column chemistry for Li isotopes followed the procedure of Seitz et al. (2004). 10–20 mg sample powder was digested in 2 ml of 1:1 HF-HNO_3 on a hot plate (140 °C) for 2–3 days. Subsequently, samples were dissolved in 6 M HCl and finally reconstituted in 6 M HNO_3 followed by chromatographic Li purification (see Seitz et al., 2004 for details). Li isotope analyses were carried out on a Neptune (Thermo Scientific) multiple collector inductively coupled plasma mass spectrometer (MC-ICP-MS) at the J.W. Goethe University (Frankfurt). The MC-ICP-MS allows simultaneous measurement of both ^6Li and ^7Li, performed at dry plasma conditions using a Cetac Aridus® nebuliser fitted with a PFA spray chamber and an ESI microconcentric-nebuliser with an uptake rate of 20 µl/s. The sample gas was dried at 160 °C before being introduced to the plasma. With the Thermo Scientific standard cones (H-Cones) an intensity of 40–50 pA, 10^{11} Ω resistor (4–5 V) for ^7Li at a 10 ng/g concentration level is achieved. The analytical blank (chemistry blank and background signal) was usually 30–20 pg (~12–20 mV on ^7Li). Sample analysis was carried out sequentially by 'bracketing' the sample with the L-SVEC standard (Flesch et al., 1973), followed by a blank measurement. The total integration time for each Li isotope measurement was approximately 4 min, following a baseline measurement (at masses 5.9 to 6.1 and 6.9 to 7.1, respectively) of approximately 1 min. Isotope compositions are expressed as per mil deviations from the NIST L-SVEC standard: $\delta^7Li = [[^7Li/^6Li]_{sample} / [^7Li/^6Li]_{L\text{-}SVEC\ standard} - 1] * 1000$. Internal precision is typically between 0.2 and 0.6‰ ($2\sigma_{mean}$) and the long-term reproducibility, determined on replicate measurements of the geological standard JB-2, is about 1.2‰ (2 SD; Supplementary Table 1).

Li concentrations of samples were determined along with the isotope measurements, by comparing the ion beam intensities with those of the 10 µg/g NIST L-SVEC standard solution. The uncertainty of this method was estimated by measuring international rock standards several times during a daily campaign. Daily precision of these concentration measurements was typically 10% (2 SD). Long-term reproducibility of the JB-2 basalt standard was 15% (2 SD, Seitz et al., 2004).

4. Analytical results

B and Li isotope data and Li concentrations of whole-rock samples are reported in Table 1, completed by B, H_2O and Cl concentrations from Vils et al. (2008), and shown in Fig. 2 versus depth.

Table 1
Li, B and Sr isotopic and Li, B and H_2O composition of samples from ODP Leg 209.

Sample	Depth	$\delta^{11}B$	±2 SD	$^{87}Sr/^{86}Sr$	±2 SD	n_{Sr}	B*	H_2O*	Li	±2 SD	δ^7Li	±2 SD	n_{Li}
	(m.b.s.f.)	(‰)		(‰)			(µg/g)	(wt.%)	(µg/g)		(‰)		
Leg 1272A													
OD 2	61.75	+32.36	0.41	0.708954	0.000010	2	58.70	16.10	0.07	0.00	−28.46	0.13	3
OD 6	76.53	+37.64	0.71	0.708873	0.000035	1	60.30	15.40	0.10	0.01	−14.25	1.37	4
OD 6/2		+37.82	0.40	n.a.			n.a.	n.a.	n.a.		n.a.		
OD 7	80.18	+37.99	0.36	n.a.			n.a.	n.a.	0.48	0.00	+7.17	0.78	4
OD 11	89.92	+35.79	0.41	0.708792	0.000010	2	53.90	16.40	0.21	0.00	−4.34	0.76	3
OD 15	99.85	+34.09	0.43	0.709130	0.000036	1	59.30	15.10	0.20	0.01	+1.24	0.89	3
OD 15/2		n.a.		n.a.			n.a.	n.a.	0.22	0.01	−0.03	1.37	4
OD 18	110.19	+38.47	0.71	0.708599	0.000027	1	59.80	15.30	0.52	0.11	+2.31	1.53	4
OD 18/2	110.19	+39.00	0.24	n.a.			n.a.	n.a.	0.52	0.08	−3.37	1.05	5
OD 22	120.05	+35.35	0.26	0.708820	0.000123	1	65.00	15.20	0.81	0.13	−0.38	0.46	3
OD 26	125.08	+39.13	0.21	0.709064	0.000022	1	61.50	13.00	0.46	0.04	−3.37	0.19	3
OD 29	129.42	+35.00	0.33	0.708983	0.000041	2	50.30	13.80	0.57	0.04	−6.83	1.47	4
OD 29/2									0.52	0.05	−4.88	1.35	4
Leg 1274A													
OD 32	0.89	n.a.		0.708792	0.000031	2	n.a.	n.a.	1.04	0.20	−6.80	1.02	4
OD 34	17.27	+34.68	0.26	0.708548	0.000010	2	31.20	12.70	0.56	0.08	−16.55	0.72	4
OD 38	27.54	+40.66	0.19	0.708536	0.000013	2	17.50	13.10	0.56	0.04	−15.57	1.06	3
OD 42	32.14	n.a.		0.707173	0.000010	3	b.d.l.	13.89	3.37	0.77	+2.84	1.76	3
OD 45	36.45	+33.69	0.48	0.708070	0.000010	2	10.40	10.90	1.13	0.19	−1.18	0.20	3
OD 48	69.79	+32.24	1.12	0.708654	0.000010	3	38.50	12.20	0.90	0.05	−12.13	1.51	3
OD 48/2		+32.61	0.33	n.a.			n.a.	n.a.	n.a.		n.a.		
OD 49	94.11	+34.11	1.07	0.708748	0.000010	3	36.60	15.00	0.28	0.06	−4.88	0.75	3
OD 49/2		+34.31	0.50	n.a.			n.a.	n.a.	n.a.		n.a.		
OD 52	146.69	+29.72	0.30	0.708539	0.000017	3	n.a.	n.a.	0.87	0.12	−0.86	1.25	4

*Data published in Vils et al. (2008), except OD 45 (same analytics as Vils et al. 2008); SD = standard deviation; *n* number of measurements; m.b.s.f. meter below sea floor; n.a. not analyzed; b.d.l. below detection limit; /2= repeated measurement, including chemistry.

4.1. Site 1272A

$^{87}Sr/^{86}Sr$ ranges from 0.708599 to 0.709130. $\delta^{11}B$ is between +32.4 and +39.1‰ (average +36.6‰), while $\delta^{7}Li$ varies from −28.5 to +7.2‰ (average −5.2‰).

$^{87}Sr/^{86}Sr$ values are close to that of seawater (0.70916, Palmer and Edmond, 1989) and show no down-hole trend (Fig. 2). $\delta^{11}B$ values show a large variation just below seawater values (+39.52‰; Smith et al., 1995). $\delta^{7}Li$ values are far from those of seawater (+31.0‰; Millot et al., 2004), but more close to those of MORB (+3.4‰; Tomascak et al., 2008). They are strongly negative in the upper part of the drill hole (−28‰), increasing to near-mantle values (+3‰) and go back to negative values (−7‰). No systematic relationship between the three isotopic systems can be observed.

4.2. Site 1274A

$^{87}Sr/^{86}Sr$ ratio varies from 0.707173 to 0.708792 (Table 1). $\delta^{11}B$ is between +29.72 and +40.66‰ (average +34.0‰), while $\delta^{7}Li$ varies from −16.5 to +2.8‰ (average −7.7‰). Sample OD 42 contains a gabbroic pocket. This magmatic influence is reflected in lower $^{87}Sr/^{86}Sr$ ratios (0.707173), higher Li contents (3.37 μg/g) and heavier $\delta^{7}Li$ +2.84‰, while B contents (<0.2 μg/g) are lower than in average serpentinites.

$^{87}Sr/^{86}Sr$ ratios are generally close to those of seawater. $\delta^{7}Li$ starts at strongly negative values and approaches MORB values with increasing depth. $\delta^{11}B$ is close to seawater values at shallow levels and tends to decrease with depth.

5. Discussion of analytical results

5.1. Relation of the observed Li and B isotope fractionation with other chemical and isotope characteristics

In general, the analyzed samples show a narrow range of $^{87}Sr/^{86}Sr$ ratios close to the seawater value, overlapping with those of other oceanic serpentinites (Mével, 2003). The high H_2O contents and $^{87}Sr/^{86}Sr$ ratios measured indicate that the sampled peridotites have extensively interacted with seawater-derived fluid (Fig. 2; Table 1). This process is also reflected by increasing B content and decreasing Li content with increasing $^{87}Sr/^{86}Sr$ ratios (Fig. 3), as a result of originally low Li (0.18 μg/g; Li, 1982) and high B (4.5 μg/g, Smith, 1995) concentration in seawater and higher concentrations in oceanic peridotites (0.7 μg/g, respectively lower 0.06 μg/g (B); Salters and Stracke, 2004). These observations are in line with the generally high degree of serpentinization occurring in the samples from both sites (up to 99%; Vils et al., 2008), although the rocks at Site 1272A are generally serpentinized to a higher degree.

This difference is reflected in the light element and Cl concentrations (Vils et al., 2008). As serpentine is the major carrier of B, H_2O and Cl, in serpentinites, the concentrations of these elements tend to higher values and scatter less at Site 1272A than at Site 1274A. As Li is mainly hosted by clinopyroxene, a primary mineral, Li concentrations are generally higher and scatter less at Site 1274A than at Site 1272A. Also, at Site 1272A, an overall decrease of H_2O, Cl, and B and an increase of Li with depth can be observed (Fig. 2), in line with the

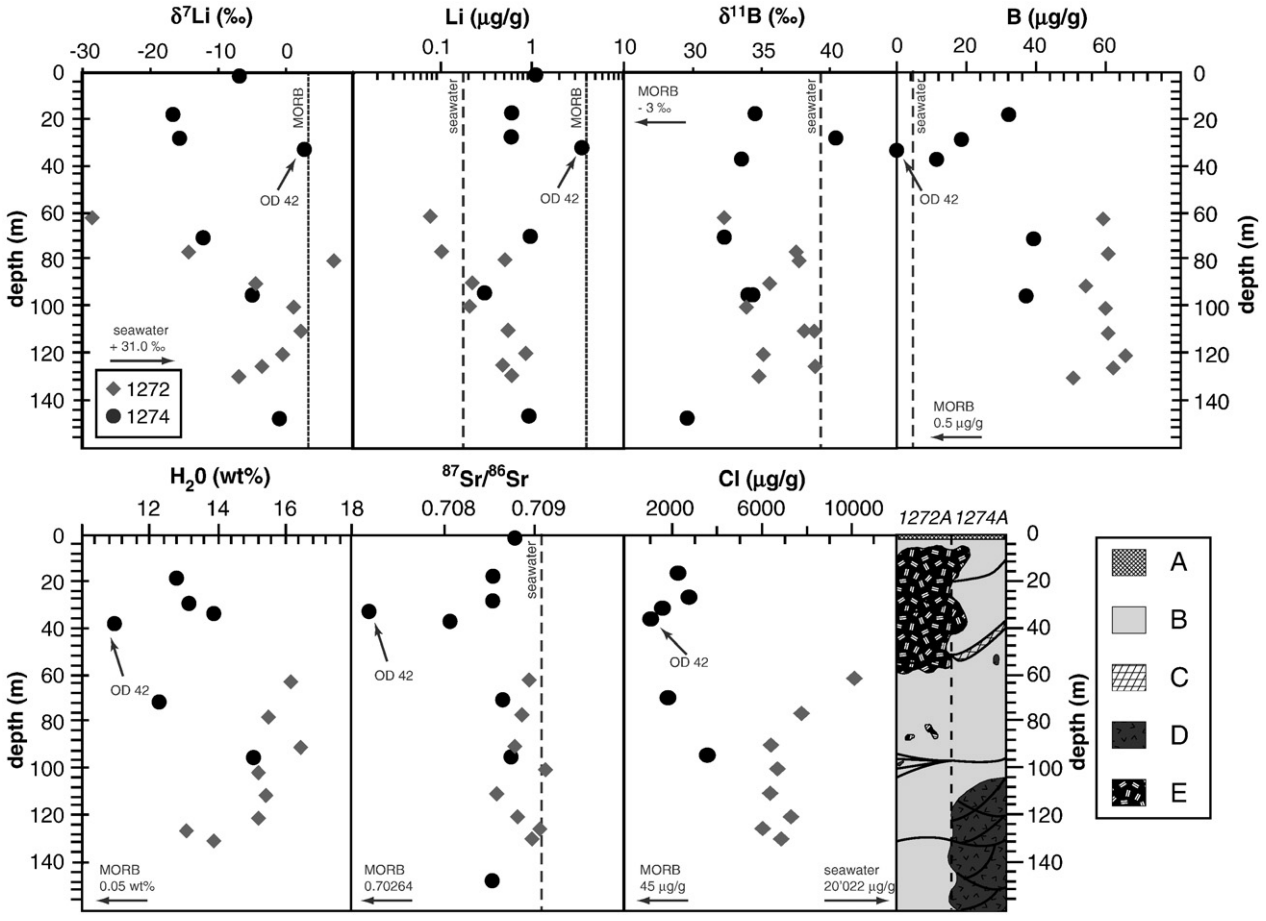

Fig. 2. Diagram showing $\delta^{7}Li$, $\delta^{11}B$, $^{87}Sr/^{86}Sr$, Li, $B^{\dagger}$, $Cl^{\dagger}$ and $H_2O^{\dagger}$ concentration versus depth for ODP Leg 209 Sites 1272A and 1274A. The data are reported in Table 1. *Data from Vils et al. (2008). Simplified lithologic log modified after Bach et al. (2004), and Vils et al. (2008). A: sedimentary cover; B: serpentinized harzburgites; D: dunite veins; E: gabbroic bodies; F: diabase. Seawater values from Palmer and Edmond (1989); Schmidt et al. (2007); Millot et al. (2004); Mid-ocean ridge basalt (MORB) values from Edmond et al. (1979), Ryan and Langmuir (1987), Rehkamper and Hofmann (1997), Tomascak et al. (2008).

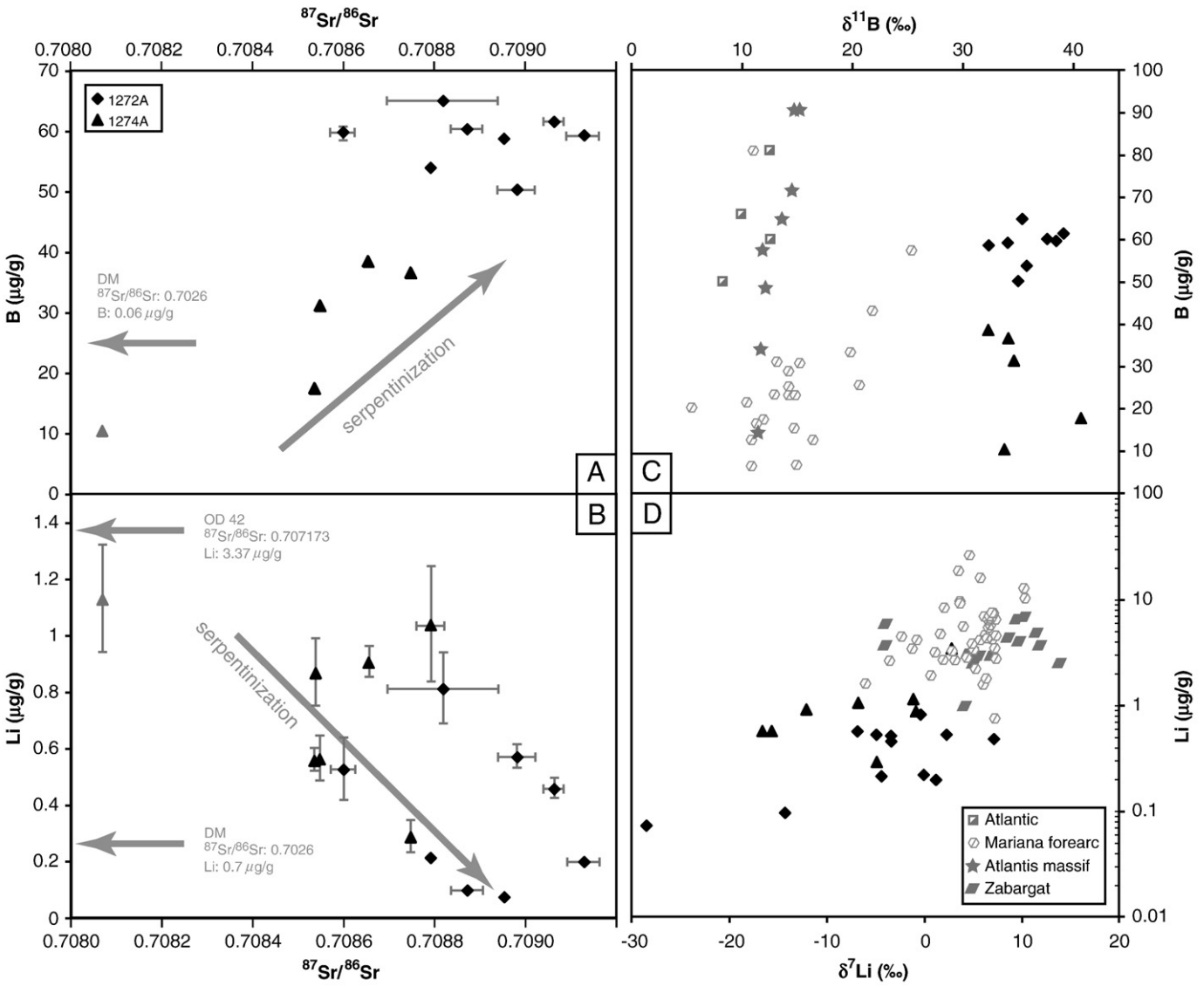

Fig. 3. B versus $^{87}Sr/^{86}Sr$ (A) and Li versus $^{87}Sr/^{86}Sr$ (B) diagrams illustrating serpentinization. If no error bar visible, errors are smaller than data point. DM = depleted mantle value (after Salters and Stracke, 2004). Additional serpentinite data are plotted for comparison: Atlantis massif (Boschi et al., 2008), diverse localities in the Atlantic (Spivack and Edmond, 1987), Mariana forearc (Benton et al., 2001, 2004), and Zabargad (Brooker et al., 2004).

observed down-hole decrease in serpentinization. The conclusion from these observations is that serpentinization added B to and removed Li from the peridotite.

The B and Li isotope data presented here and their trends with B and Li concentrations (Fig. 3) indicate that isotope fractionation occurs during serpentinization. For Site 1274A, there is a positive correlation between Li concentrations and δ^7Li (Fig. 3). The strongly negative δ^7Li values and their trend towards less negative values in the uppermost part of Site 1272A are very likely due to the high degree of serpentinization (high H_2O, high $^{87}Sr/^{86}Sr$ ratios and low Li content in the sample), related to fluids entering through a fault gouge at 60 m.b.s.f. (meter below seafloor). The less negative δ^7Li values in the lower part of the borehole (and the higher Li concentrations) can be explained by the presence of larger fractions of clinopyroxene as the degree of serpentinization decreases from 99 to 70% and clinopyroxene occurrence increases. These observations indicate that during serpentinization, ^{7}Li is preferentially leached from the rocks.

There is no simple correlation between δ^{11}B and B concentrations. On the average, the spread in δ^{11}B is larger and values tend to be lighter at Site 1274A (lower average degree of serpentinization) compared to Site 1272A (higher average degree of serpentinization; Figs. 2 and 3). Also, when omitting the data points for sample OD 42 (crosscut by a magmatic vein), δ^7Li and δ^{11}B show a negative down-hole correlation for Site 1274A at which relations are not complicated by a fault gouge (Fig. 2). These observations suggest that during serpentinization, ^{11}B is preferentially added to peridotites.

Although on δ^{11}B and δ^7Li data of serpentinites are still scarce, this work provides δ^{11}B values significantly higher (+29.7 to +40.7‰) than those found so far for any serpentinized oceanic peridotite (Fig. 3). Among the δ^7Li values obtained in this work (−28.5 to +7.2‰) are the most negative ones found so far for serpentinized oceanic peridotite, and our entire dataset tends to more negative values than previously found (Fig. 3).

5.2. Constraints on seawater–peridotite interaction for ODP Leg 209

During peridotite–seawater interaction, the observed B and Li isotope fractionation is controlled by temperature, by pH (for B) and by water/rock ratio. Kakihana and Kotaka (1977) calculated the fractionation factor between BOH_3–BOH_4 in a fluid ($\alpha_{3/4}$ = 1.0193 at 300 K). New ab initio molecular orbital calculations for boron isotope fractionation on boric acids and borates of Liu and Tossell (2005) showed that the B $(OH)_3$–$B(OH)_4$ isotope fractionation is higher ($\alpha_{3/4}$ = 1.0245 at 300 K),

moreover there is also a fractionation factor to consider between $B(OH)_4^-$ in aqueous solution and BO_4 in silicates. Combining the two fractionation factors, we obtain a dataset illustrating the B isotope fractionation between seawater and silicates (≈rock) as a function of temperature and pH (Supplementary Table 2). Best-fit lines through the calculated values are shown in Fig. 4. For example, assuming an average serpentinization temperature for oceanic mantle rocks of 200 °C and seawater pH (8.2), we obtain $\Delta^{11}B_{seawater-silicate} = -19‰$ (Fig. 4). If pH in a fluid is lower than seven, only $B(OH)_3$ is stable, while at pH higher than ten, there is only $B(OH)_4$ (Spivack and Edmond, 1987; Boschi et al., 2008). Thus, the fractionation factors on the curves for pH seven and pH ten in Fig. 4 represent minima and maxima, respectively.

For ODP Leg 209 Sites 1272A and 1274A, positive $\delta^{37}Cl$ values (structurally bond and water soluble Cl) at Site 1272A and Site 1274A identify a seawater-buffered fluid as primary serpentinization fluid under low T-conditions (Barnes and Sharp, 2006; Barnes et al., 2009). Additionally, $\delta^{18}O$ isotopic composition and mineralogy indicate serpentinization temperatures between 150 °C and 250 °C (Bach et al., 2004; Alt et al., 2007; Barnes et al., 2009). We consider 200 °C as average serpentinization temperature at both sites. If we assume a single-stage seawater–peridotite equilibration, pH should be that of seawater (8.2). $\delta^{11}B$ values obtained in this work (+29.7 to +40.7‰) result in $\Delta^{11}B_{seawater-rock}$ values of +2 to −10‰. Using the fractionation factor of Liu and Tossell (2005) and considering a single-stage equilibrium process at pH of 8.2, temperature must have been between 400 and 1000 °C which is not realistic. Moreover, Boschi et al. (2008) showed that during low-temperature seawater–rock interaction (0–25 °C, pH 7.5–8.5), $\delta^{11}B$ in an equilibrated rock reaches a maximum value of +7‰. This is similar to values of dredged serpentinites from the different localities in the Atlantic Ocean (+8.3 to +12.6‰; Spivack and Edmond, 1987). Additionally, low δD values at Site 1272 and Site 1274 suggest non-equilibrium conditions with seawater (Barnes et al., 2009). Hence, a single-stage equilibrium process, as is probably the case for weathering of peridotite on the ocean floor, is not a realistic model for seawater–peridotite interaction at Sites 1272A and 1274A.

It seems more reasonable to assume that batches of seawater penetrate into the oceanic plate and continuously evolve during interaction with the surrounding rocks (in our case peridotite). Such a process is in line with the composition of fluids emerging at oceanic hydrothermal vent sites hosted by ultramafic rocks (e.g. Li: 0.33 to 2.38 µg/g for Rainbow, Logatchev and Lost City hydrothermal fields; B: 0.34 to 3.69 µg/g for Logatchev and Lost City; Douville et al., 2002; Schmidt et al., 2007) which may be enriched or depleted in B or Li compared to seawater (0.18 µg/g Li, 4.5 µg/g B; Quinby-Hunt and Turekian, 1983; Schmidt et al., 2007). The chemical variability of such hydrothermal fluids was explained by a vent site evolution model (McCaig et al., 2007) in which single hydrothermal fields correspond to different evolution stages of low-angle detachment faults where emerging fluids interact with different rock types to different degrees (mafic and ultramafic lithologies). Hydrothermal fields have various pH (2.8 to 9.8; e.g. Kelley et al., 2001; Douville et al., 2002), depending on their solid buffer (pure ultramafic lithologies, pure basalt lithologies or mixtures of the two). Theoretical modelling of the behaviour of B during serpentinization revealed that changing pH during serpentinite formation at the Atlantic massif could be responsible for the observed $\delta^{11}B$ (Boschi et al., 2008).

Fractionation of Li isotopes does not seem to be dependent on pH, but is sensitive to temperature and pressure (e.g. Wunder et al., 2006). Pressure, however, plays no role for samples dredged or drilled from the ocean floor. Estimation of Li fractionation due to clay formation in weathered basalts ranges from −17 (4 °C) to −3‰ (350 °C; Chan et al., 1992; Chan et al., 1993). Recent experiments on incorporation of Li on the octahedral side of Mg-rich clay minerals showed strong temperature dependencies of Li fractionation (e.g. 200 °C, $\Delta^7Li = -3.6‰$; Vigier et al., 2008). On serpentinites from the Southwest Indian Ridge, Decitre et al. (2002) obtained Li isotopic compositions lighter and heavier than the unaltered rocks. The authors interpreted this variation as internal recycling of Li from the hot MORB into the progressively forming serpentinites, rather than a direct exchange with seawater.

Calculation of the ocean δ^7Li budget by Huh et al. (1998) led to the conclusion that there needs to be a mineral phase in the oceans acting as a sink for Li, with $\Delta^7Li_{seawater-phase} = -23‰$. Adsorption and desorption experiments on phyllosilicates implied that $\Delta^7Li_{seawater-phase}$ is $> -20‰$ (Zhang et al., 1998). These statements are in line with recalculation of the δ^7Li content of the ocean, based on the assumption that clay phases are the major Li sink, leading to $\Delta^7Li_{seawater-clay}$ between −12 to −21‰ (Vigier et al., 2008). As serpentine is also a phyllosilicate, fractionation factors for Li similar to those of clay minerals seem reasonable.

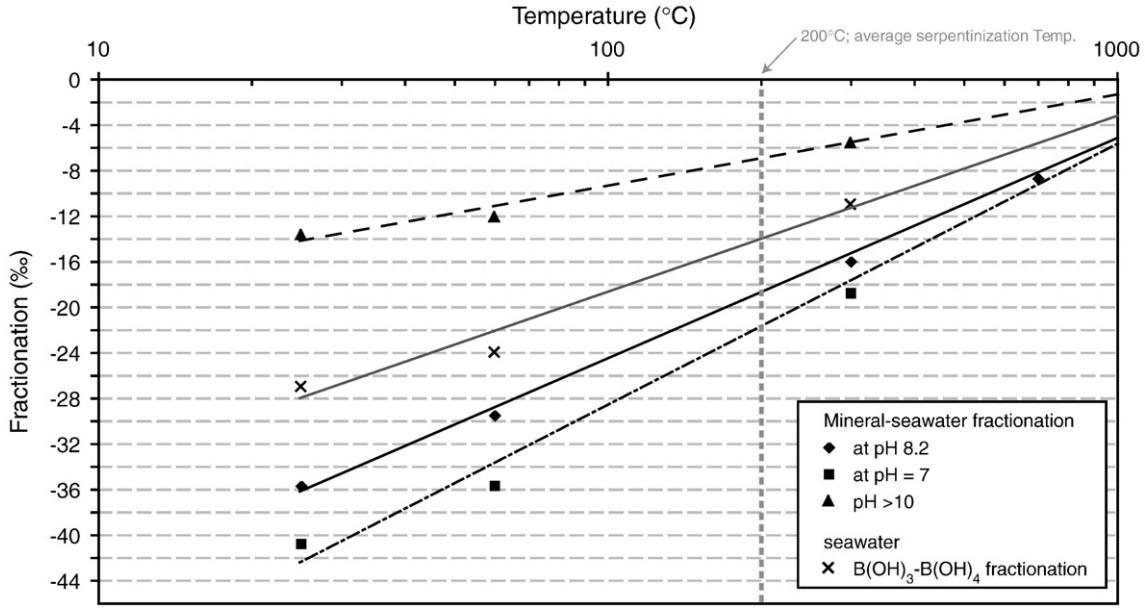

Fig. 4. Boron isotope fractionation versus temperature diagram (data from Liu and Tossell, 2005) showing the influence of pH on boron isotopes. Average serpentinization temperature chosen after Bonatti et al. (1984) and Bach et al. (2004).

6. Modelling seawater and rock evolution during fluid–rock interaction

In the following, we model the evolution of seawater and the composition of coexisting rock in terms of $\delta^{11}B$ and $\delta^{7}Li$ values during continuous fluid–rock interaction in a closed system. Based on our previous results (Vils et al., 2008), we assume that during this process B is added to peridotite through serpentinization while Li is leached from the rock. The other parameters, e.g. $\delta^{11}B$ and $\delta^{7}Li$ values of seawater and peridotite, and fractionation factors, are given in the Appendix.

6.1. Results

In Fig. 5, the modelled process of fluid–rock interaction is illustrated by the stepwise evolution of a fluid batch reacting with ultramafic rocks. With each step, 10% of the fluid is adsorbed onto and integrated into the surrounding rocks. The fluid acquires increasingly heavy $\delta^{11}B$ (Fig. 5A, B). The rock in equilibrium with such a fluid follows the same trend, if the fractionation factor is kept constant according to data from Fig. 4. The influence of temperature at constant pH is shown in Fig. 5A. At low reaction temperatures, fluids become more quickly enriched in ^{11}B and end up with higher $\delta^{11}B$ than at high temperatures. The influence of pH at constant temperature is shown in Fig. 5B. As low pH favours the presence of trigonally coordinated B and thus ^{11}B, low-pH fluids become more quickly enriched in ^{11}B and end up with higher $\delta^{11}B$ than high-pH fluids. Fig. 5A and B show that fluids in equilibrium with rocks from ODP Leg 209 should have been isotopically heavier than seawater. Applying a fractionation of -19‰ at serpentinization temperature of 200 °C on a batch of seawater (pH = 8.2), fluids in equilibrium with rocks of ODP Leg 209 should have had $\delta^{11}B$ of $+50$ to $+60$‰ (Fig. 5B).

Fig. 5C shows the evolution of $\delta^{7}Li$ in a fluid and coexisting rock during water–rock interaction. The line in Fig. 5C ($\Delta^{7}Li = -4$‰; corresponding to seafloor weathering) does not intersect with the field outlined by samples from ODP Leg 209. Therefore, as already deduced from the B isotope systematics, seafloor weathering seems an unlikely process for the studied samples. In contrast, the line calculated using the fractionation of $\Delta^{7}Li = -21$‰ proposed by Vigier et al. (2008) intersects the data field for the ODP Leg 209 samples which have extremely light $\delta^{7}Li$. Applying a fractionation of -21‰, fluids in equilibrium with rocks of ODP Leg 209 should have had $\delta^{7}Li$ of -2 to $+12$‰ (Fig. 5C).

The modelling results from both isotope systems are consistent. First, they exclude that the serpentinites of ODP Leg 209 represent seafloor weathering or have been reequilibrated during such an event. This result is in line with the conclusions from B and Li concentrations (whole rock and minerals; Vils et al., 2008). Second, the model further shows that the peridotites of ODP Leg 209 most likely acquired their extremely heavy $\delta^{11}B$ and their extremely light $\delta^{7}Li$ by reaction with an evolved fluid that had already exchanged 50–70% of its B and 60–80% of its Li with ultramafic rocks (Fig. 5).

6.2. Discussion

The measured isotope data are consistent with our model calculations, however, there may be alternative processes that could generate extremely heavy $\delta^{11}B$ and extremely light $\delta^{7}Li$ in serpentinized peridotites. The above-mentioned model is only valid under equilibrium conditions and closed-system behaviour. The penetrating fluid may not have been saturated in Li or B. In this case, even larger fractionation factors would have to be applied.

A general uncertainty concerning the $\delta^{7}Li$ and $\delta^{11}B$ of serpentinite arises from the assumption that Li and B are incorporated into the mineral structure where they replace Mg^{2+} and Fe^{2+} (Li) or Si^{4+} on the tetrahedral site (B). Phyllosilicates can additionally contain small cations in interlayers. No additional fluid–mineral fractionation should occur in this case and therefore, such interlayer Li or B should reflect the isotopic composition of the fluid. Published data on pore water (average + 17‰ $\delta^{11}B$; Wei et al., 2005) at pH>12 and coexisting serpentine clasts (average + 11‰ $\delta^{11}B$; Benton et al., 2001) from Mariana forearc are in line with the fractionation of -7‰ predicted in Fig. 4, arguing for structurally bond B rather than for interlayer B. A micro-Raman study on serpentine from ODP Leg 209 and ophiolitic serpentine revealed that in ophiolitic serpentine B and Si^{4+} correlate and that B must therefore be structurally bond (Pelletier, 2008). The correlation was less clear for oceanic serpentine, probably due to the very small serpentine grain size. Additionally, neither values from Lost City (Boschi et al., 2008) nor our data (this paper) represent direct seawater–rock interaction, which would be expected for interlayer B. As B seems to be structurally bond, fractionation between fluid and minerals is very likely to occur. Therefore, we used the fractionation factors shown in Fig. 4 for modelling seawater evolution during fluid–rock interactions (Fig. 5).

The modelled $\delta^{11}B$ of the fluid in equilibrium with ODP Leg 209 serpentinites tends towards higher values ($+50$ to $+60$‰) compared to those published for hydrothermal vent sites. Fluids emerging at hydrothermal fields have $\delta^{11}B$ between $+10$ and $+37$‰ (Palmer, 1991). Heavier values are reported for sediment-starved systems ($+26.7$ to $+36.8$‰) compared to sediment-hosted systems ($+10.1$ to $+11.5$‰; Palmer, 1991). At the Lost City hydrothermal field (Atlantic massif), hosted by ultramafic rocks, $\delta^{11}B$ values of $+25$‰ are reported for end member fluids (Boschi, 2006). The results of Raleigh distillation models applied to the Lost City hydrothermal vent system predict, however, that at 100 °C, initial seawater should acquire $\delta^{11}B$ of $+120$‰ due to pH increase during serpentinization (Foustoukos et al., 2008). Also, at Lost City, hydrothermally precipitated aragonite (which incorporates preferably tetrahedrally coordinated B at low fractions; Sen et al., 1994; Hemming et al., 1995) has $\delta^{11}B$ up to $+53$‰ (Boschi, 2006), suggesting equilibration to fluids with $\delta^{11}B$ of around $+62$‰ (fractionation 9‰; at 100 °C; Fig. 4).

For Lost City, the discrepancy between the modelled high-^{11}B fluid composition (supported by the $\delta^{11}B$ of aragonite) and the measured fluid composition may be explained by the presence of brucite. Considerable quantities of brucite have been found at Lost City and are invoked by Boschi (2006) to be the cause of relatively low-^{11}B fluids. Based on the work of Pokrovsky et al. (2005), Foustoukos et al. (2008) suggested that brucite may preferentially incorporate trigonal B and hence lower the $\delta^{11}B$ of the coexisting fluid.

From ODP Leg 209 Sites 1272A and 1274A, brucite has been described as an accessory phase (Bach et al., 2004). Very likely, this is not sufficient to lower the $\delta^{11}B$ value of the reacting fluid. It may be more reasonable to consider our assumption of constant pH for the model as too simple. Using phase equilibria constraints, several authors (e.g. Frost and Beard, 2007) have predicted that pH should become increasingly alkaline during serpentinization reactions at very low temperatures. According to the model of Foustoukos et al. (2008), the pH effect is less pronounced at temperatures of 200 °C, relevant for ODP Leg 209 samples. At these conditions, the $\delta^{11}B$ of a serpentinizing fluid would be $+50$‰ (their Fig. 7), corresponding to our modelled values.

Published $\delta^{7}Li$ values of hydrothermal fluids range from $+2.6$ to $+10.7$‰ (Chan and Edmond, 1988; Chan et al., 1992; Chan et al., 1993; Foustoukos et al., 2004). In particular, the MARK hydrothermal field (23°N) north of the Fifteen–Twenty fracture zone has $\delta^{7}Li$ values varying between $+6.3$ and $+8.0$‰ (Chan et al., 1993). All published data agree with our modelled fluid composition ($\delta^{7}Li$ of -2 to $+12$‰; Fig. 5C). A similar evolution of Li in seawater through serpentinization is also invoked by Decitre et al. (2002) for serpentinites from the Southwest Indian Ridge. However, their in-situ analyses of serpentine ($\delta^{7}Li$ up to $+25.5$‰) suggest that prior to serpentinization, fluids are

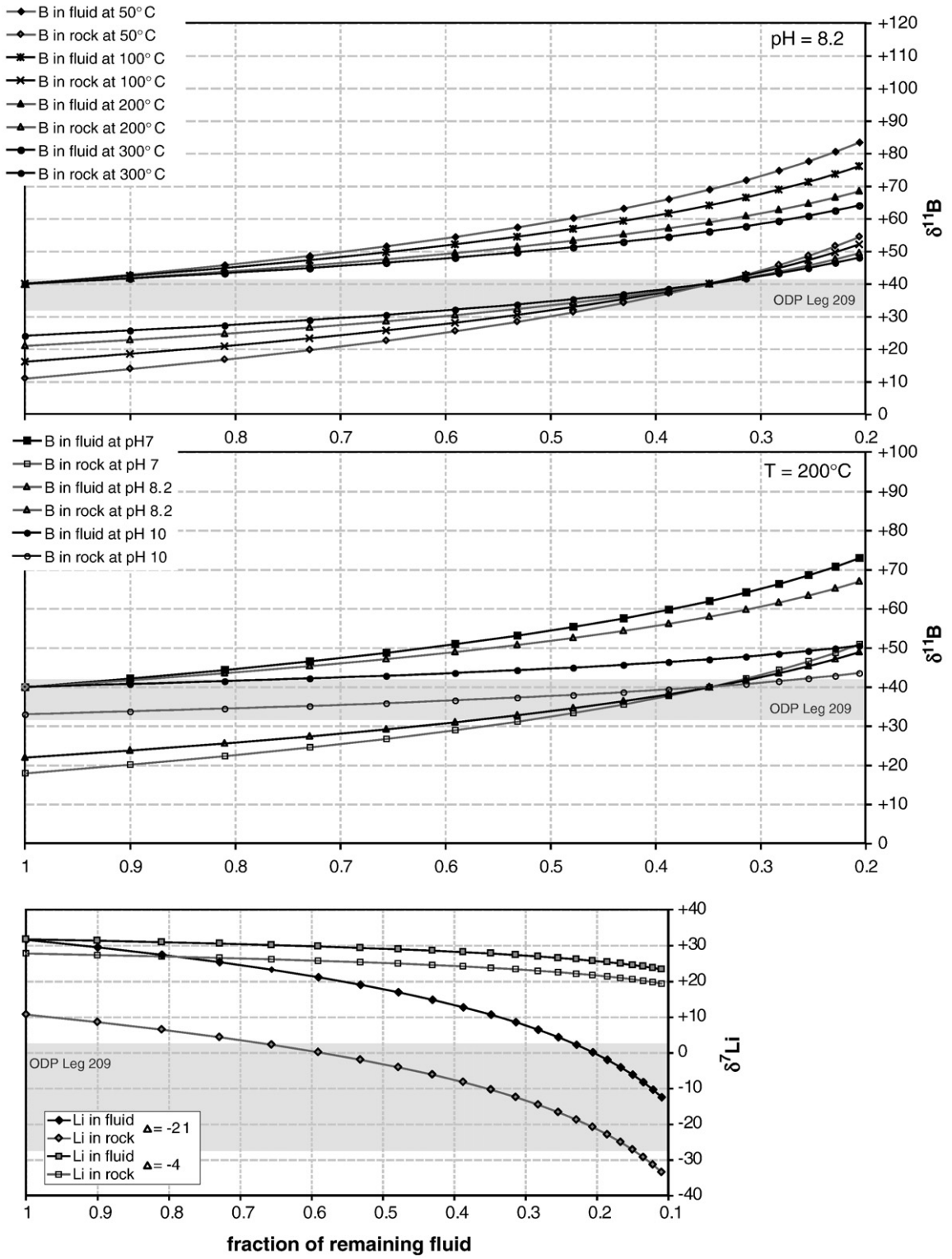

Fig. 5. Model of isotopic evolution of fluid and corresponding rock (in equilibrium) during closed-system stepwise fluid–rock interaction ($\delta_n = \delta_{(n-1)} * 0.1 * \Delta$; n: step number). See Appendix for further explanations. A: Results for $\delta^{11}B$ at different temperatures at constant pH (8.2). B: Results for $\delta^{11}B$ at different pH values at constant T (200 °C). C: Results for $\delta^{7}Li$ using different fractionations (Chan et al., 1992; Vigier et al., 2008).

heated up in the oceanic plate and doped with Li and δ^7Li through reaction with basalt.

7. Influence of water/rock ratios on B and Li isotopic composition

Similar abundances of strontium in the mantle (9.8 μg/g; Salters and Stracke, 2004) and in seawater (7.8 μg/g; Quinby-Hunt and Turekian, 1983) and the absence of fractionation of strontium isotopes during fluid–rock interaction leads to a linear mixing line between $^{87}Sr/^{86}Sr$ ratios of mantle (0.7025, Rehkamper and Hofmann, 1997) and seawater (0.70916, Palmer and Edmond, 1989). $^{87}Sr/^{86}Sr$ ratios are therefore a useful tool to quantify the fluid flow through a sample (expressed as water/rock ratio). We calculated water/rock ratios (N) for ODP Leg 209 samples assuming a closed system and a 'single-

pass-model'. We used Eq. (1) after Taylor (1977) and McCulloch et al. (1980), assuming $\delta_r^f = \delta_w^f - \Delta$ and for $^{87}Sr/^{86}Sr$ $\Delta = 0$. Results and input values are reported in Table 2.

$$N = \left(\frac{\delta_r^f - \delta_r^i}{\delta_w^i - \delta_w^f}\right) \times \frac{c_r^i}{c_w^i} \quad (1)$$

r corresponds to rock, w to water or fluid, Δ to fractionation, f to final and i to initial composition. Calculation of N for ODP Leg 209 showed moderately high average N of 39. Values for Site 1272A (13–273) are higher than for Site 1274A (3–21), which is in line with the lower primary mineral content, the higher H_2O contents and the higher serpentinization degree at Site 1272A compared to Site 1274A (Vils et al., 2008). Opposed to unaltered MORB (0.7025; Rehkamper and Hofmann, 1997), the serpentinites of ODP Leg 209 have exchanged a large fraction of their Sr with fluid (70–100%; $100 \times [^{87}Sr/^{86}Sr_{sample} - ^{87}Sr/^{86}Sr_{MORB}] / [^{87}Sr/^{86}Sr_{seawater} - ^{87}Sr/^{86}Sr_{MORB}]$ after (Davies et al. 2003; Table 2), indicating extensive fluid–rock interaction. Similar water/rock ratios (18–234) and fractions of exchanged Sr (96–100%) were reported for Atlantis Massif serpentinites (Delacour et al., 2008). Spooner et al. (1977) and Delacour et al. (2008) concluded that during serpentinization, Sr was only locally mobilized (leached from primary minerals and precipitated in secondary minerals), and no Sr was added or removed. Similar exchange mechanisms seem to control the $^{87}Sr/^{86}Sr$ ratios of altered oceanic crust (e.g. Spooner et al., 1977).

Li, B and Sr isotope systematics from ODP Leg 209 indicate extensive seawater interaction, and the closed-system calculation showed high water–rock ratios (Table 2), which is in line with the high H_2O content of the samples (Vils et al., 2008). In hydrothermal systems at mid-ocean ridges, fluid–rock interaction is continuous. Nevertheless, emerging fluids at hydrothermal vents show highly variable Sr contents and $^{87}Sr/^{86}Sr$ ratios (3.5–24 μg/g; 0.70279–0.70997, respectively; Albarède et al., 1981; Palmer and Edmond, 1989). During its passage through the rock column, seawater continuously exchanges elements with the surrounding rock and hence changes its isotopic composition. As shown above, the $\delta^{11}B$ and δ^7Li data of ODP Leg 209 are coherent with such a fluid evolution. In order to model coupling between water/rock ratio and the isotopic evolution of a fluid during fluid–rock interaction, we used a stable isotope balance equation (Eq. (2); after Pennisi et al., 2000), which is a derivative of Eq. (1) assuming $\delta_r^f = \delta_w^f - \Delta$ (Eq. (2.1)), solved for final fluid composition.

$$\delta_w^f = \frac{N*\delta_w^i + \frac{C_r}{C_w}*\left(\delta_r^i + \Delta_{w-r}\right)}{N + C_r / C_w}. \quad (2)$$

Input values and results are reported in Table 2. Fractionation between fluid and rock are kept constant and rock in equilibrium with fluid was calculated using Eq. (2.1). Applying equation Eq. (2) to the Li and B isotopic system shows that already low values of N lead to near-final fluid composition for $\delta^{11}B$, while δ^7Li change requires higher N (Table 2 and Fig. 6). The range produced from minimal and maximal fluid composition (input values from Fig. 5B and C) cover most of the data points measured at ODP Leg 209, while seafloor weathering (equilibrium with seawater) leads to lighter $\delta^{11}B$ and heavier δ^7Li (Fig. 6). Data from ODP Leg 125 (Mariana forearc) are probably not derivates of similar fluid evolution processes, as high serpentinization is not coherent with low N (Fig. 6) and fluid originates in the dehydrating subducting plate (e.g. Benton et al., 2001).

As shown before, Li and B isotopes are both highly sensitive to fluid–rock interaction. However, they seem to be decoupled with respect to water/rock-ratios, B requires only lower water/rock-ratios to adapt its isotopic composition than Li (Fig. 6). A minimum water/rock-ratio of 0.13 (corresponding to ~0.1 water/rock-ratio in Fig. 6) is required to stoichiometrically transform ultramafic rock into serpentinite (Sakai et al., 1990). Fig. 6 shows that enrichment of B in the rocks takes place mostly between a water/rock ratio of 0.13 and 1, leading to

Table 2
Calculation of water–rock ratios, isotopic evolution and input parameters.

Eq. (1)	Leg 1272A	W/R	Ex.	Leg 1274	W/R	Ex.
	OD 2	39	97	OD 32	21	94
	OD 6	27	96	OD 34	12	91
	OD 11	21	94	OD 38	12	90
	OD 15	273	100	OD 42	3	70
	OD 18	13	91	OD 45	6	83
	OD 22	23	95	OD 48	15	92
	OD 26	85	99	OD 49	19	94
	OD 29	45	97	OD 45	12	91

Eq. (2)	N (=W/R)	($\delta^{11}B$) w,f	(δ^7Li) w,f	($^{87}Sr/^{86}Sr$) w,f
	0.001	16.4	25.0	0.70869
	0.01	33.4	25.0	0.70892
	0.1	54.6	25.0	0.70901
	0.5	58.8	25.1	0.70902
	1	59.4	25.2	0.70902
	10	59.9	25.7	0.70903
	20	60.0	25.8	0.70903
	50	60.0	25.9	0.70903
	100	60.0	26.0	0.70903
	1000	60.0	26.0	0.70903

Input parameters		Boron	Lithium	Strontium
Eq. (1)	c, i, r (μg/g)	0.06[§]	0.7[§]	9.8[§]
Eq. (1)	c, i, w (μg/g)	4.5[$]	0.18[£]	7.8†
Eqs. (1) and (2)	c, i, r/c, i, w	0.013	3.89	1.26
Eqs. (1) and (2)	δ w, i (max)	+60*	+26*	0.70916¢
Eqs. (1) and (2)	δ w, i (min)	+51*	−8*	0.70916¢
Eqs. (1) and (2)	δ r, i	−3#	+4′	0.703[§]
Eq. (2)	$\Delta w-r$	−19*	−21*	0

Eqs. (1) and (2) see text for details. N = water–rock ratio; Ex. = % of Srisotopic exchange; c = concentration (μg/g); i = initial; r = rock; w = fluid; δ = isotopic value or ratio; Δ = fractionation water–rock; [§]Salters and Stracke (2004); [$]Smith (1995); [£]Li et al. (1982); [†]Quint-Hunt et al. (1993); [#]Hart et al. (1999); [¢]Palmer and Edmond (1989); ′Tomascak et al. (2008); *values from Figs. 4 and 5.

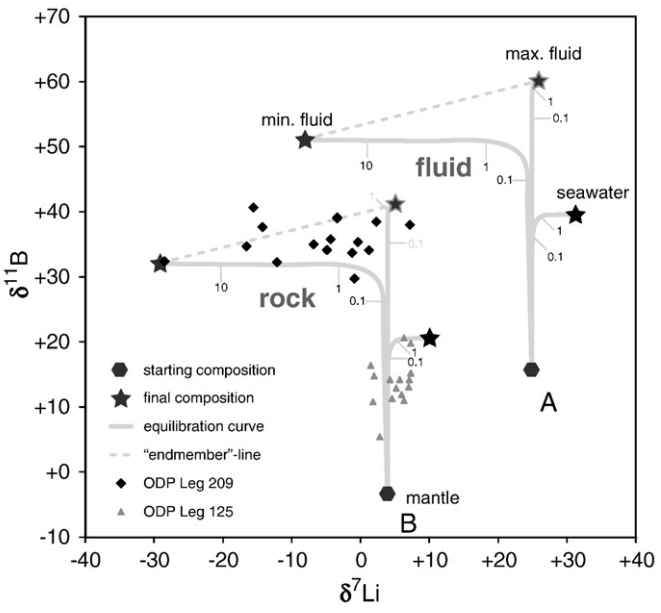

Fig. 6. δ^7Li versus $\delta^{11}B$ diagram showing the data points of ODP Leg 209 and ODP Leg 125 (Mariana forearc; Benton et al., 2001; Benton et al., 2004). Lines correspond to modelled fluid–rock interaction using the equation of Pennisi et al. (2000). They show the evolution of δ^7Li and $\delta^{11}B$ in fluid (A) and coexisting rock (B) at different water/rock ratios. Input values are reported in Table 2; 'min. fluid' and 'max. fluid' curves correspond to minimal and maximal fluid values from Fig. 5 to explain ODP Leg 209 dataset (e.g. for δ^7Li initial fluid: +26 and −8‰).

heavier $\delta^{11}B$. On the contrary, Li is leached out (or enriched) in the rocks if water/rock ratio is >1, leading to lighter $\delta^{7}Li$ (or heavier $\delta^{7}Li$ in the case of enrichment). The reason for this decoupling may lie in the difference in initial fluid and rock Li and B concentrations (large difference between fluid and rock for B compared to Li, Table 2). Additionally, the presence of magnetite in serpentinite indicates availability of Fe^{3+} through oxidation reactions during serpentinization, which may limit Li substitution for Fe^{2+}. In experiments by Seyfried and Dibble (1980) on seawater–peridotite interaction (at 300 °C and 500 bars), the fluid phase became enriched in Si at the beginning, but Si was later removed from the solution by incorporation into secondary minerals. At the same time B contents of the solution decreased, but get mostly incorporated during quenching. In contrast, Mg concentrations seemed to decrease continuously from the beginning of the experiment, and might in this case incorporate Li into the secondary minerals as proposed by Fig. 6 with seawater as final fluid composition. The different behaviour of Si and Mg probably strongly affects the Li and B incorporation/expulsion into/of the atomic structure of serpentine and therefore the isotopic compositions. Concluding, there may be crystal-chemical and kinetic reasons why B adapts its isotopic composition already at lower water/rock ratios in contrast to Li.

8. Implications for the global B and Li cycle

Our data have potential impact on the issue of light element recycling and isotope fractionation in subduction zones. The $\delta^{11}B$ and $\delta^{7}Li$ obtained on the samples from ODP Leg 209 are the heaviest and the lightest, respectively, found so far for serpentinized peridotites from the oceanic domain. Subduction of oceanic mantle with such features could potentially control the composition of slab fluids, particularly in cases where magmatic oceanic crust is largely absent. Subduction and dehydration of oceanic crust should produce slab fluids that have heavy $\delta^{11}B$ and $\delta^{7}Li$ and high B (and Li) concentrations. In contrast, fluids released from a subducting ODP Leg 209-type mantle should probably have considerably lighter $\delta^{7}Li$ and heavier $\delta^{11}B$, very low Li and variably high B concentrations. Even if there is a magmatic crust, the B isotopic composition of serpentinized mantle should control the composition of slab fluids, as it is the principal carrier of B, especially if only its upper part is dehydrated (Vils et al., 2008). For Li, our study showed that the extremely light $\delta^{7}Li$ values are coupled to very low Li contents of serpentinites. Thus, it is unlikely that the extremely light $\delta^{7}Li$ as found in ODP Leg 209 serpentinites are transferred to slab fluids. Even a small fraction of magmatic or sedimentary crust would strongly dominate the Li budget.

An important question to ask is if oceanic mantle with B and Li element and isotope characteristics such as those observed in ODP Leg 209 is likely to enter a subduction zone. As oceanic lithosphere moves away from the spreading center and cools, serpentinized peridotites may attain isotopic equilibrium with seawater if they have sufficient time. One argument in favour of this hypothesis may be that $\delta^{11}B$ of dredged serpentinites is lighter (+8.3 to +12.6‰; Spivack and Edmond, 1987) than that of drilled serpentinites from ODP Leg 209. On the other hand, slow reaction kinetics at such low temperatures could impede re-equilibration. Permeability experiments on peridotites showed that at 100 °C, a 100 m thick mantle column is completely serpentinized after 3 Ma, and at 34 °C after ~160 Ma (MacDonald and Fyfe, 1985). Thus, given that the average age of an oceanic plate before being subducted is 75 Ma, it seems unlikely that low-temperature re-equilibration affects a considerable part of the serpentinized oceanic mantle.

Another point to consider is that serpentinization related to slab bending (Ranero et al., 2003) might influence the B and Li isotope characteristics of the serpentinized mantle. Serpentine and serpentinite formed at these conditions should have lighter $\delta^{11}B$ than ODP Leg 209 samples if they equilibrate with seawater at fairly low temperatures. However, plate bending and subsequent subduction are likely to be faster than re-equilibration of B and Li isotopes, given the low velocity of serpentinization at low temperatures. Unfortunately, there are no B and Li isotope data from this geodynamic setting. Serpentinized peridotites from the Mariana forearc mantle wedge show significant enrichment in ^{7}Li ($\delta^{7}Li$ of +10.3‰) and ^{11}B ($\delta^{11}B$ of +25.3‰), presumably due to reaction with subduction-related fluids (Benton et al., 2001; Benton et al., 2004). However, these data from a mantle wedge beneath the upper plate of a subduction zone cannot be compared to our data from ODP Leg 209. In a subduction scenario, the latter should represent the mantle of the lower plate which should a-priori not be exposed to slab fluids.

A further question to be asked is in what way the B and Li chemical and isotopic composition of ODP Leg 209 is representative of the Earth's mantle. Most of today's subducted oceanic crust is of the fast-spreading ridge type, with magmatic crust dominating the chemical and isotopic budget. However, the Jurassic/Cretaceaous Tethys was largely produced by slow-spreading ridges. Therefore, most obducted and metamorphosed oceanic plates exposed on-land are relicts of slow-spreading ridges, and their chemical and isotopic signature should be similar to ODP Leg 209 (e.g. Pindos ophiolite; Pelletier et al., 2008) — if not changed by processes in the continental crust. Accordingly, the B and Li chemical and isotopic composition of ODP Leg 209 should be present in Jurassic/Cretaceous oceanic plate that was subducted in Eocene times.

9. Conclusions

1) Serpentinization of peridotite at ODP Leg 209 Sites 1272A and 1274A enriched the rock in B and ^{11}B and depleted it in Li and ^{7}Li. Serpentinization thus led to a considerable fractionation of B and Li isotopes.
2) The ODP Leg 209 rocks and the fluids calculated to be in equilibrium with them have the heaviest $\delta^{11}B$ and the lightest $\delta^{7}Li$ reported so far. The peridotites were neither serpentinized by weathering under seafloor conditions nor exposed to the latter after serpentinization. Most likely, serpentinization was not a single-stage process, but a continuous process of fluid–rock interaction, with the original seawater changing its B, $\delta^{11}B$, Li and $\delta^{7}Li$ signature upon reaction.
3) Moderate water/rock ratios (~39) calculated from the Sr isotopic composition of the samples imply an infinite rock reservoir, but limited seawater availability. Low water/rock ratios (~1) already lead to near-final $\delta^{11}B$ composition of the rock, while $\delta^{7}Li$ is modified considerably only at higher water/rock ratios. This suggests that B exchange during serpentinization is faster and easier than Li exchange.
4) There is a fair chance that extremely heavy $\delta^{11}B$ in serpentinized oceanic mantle can be transported into subduction zones, as the B budget of the plate is dominated by serpentinites. On the contrary, extremely light $\delta^{7}Li$ in the oceanic mantle is unlikely to survive as the Li budget is dominated by the oceanic crust, even at small fractions.

Acknowledgements

The authors would like to thank Arjan Dijkstra, Chiara Boschi, Andrea Dini, Tim Elliott and Othmar Müntener for fruitful discussions, which helped to improve the manuscript. The authors appreciated the reviews of Paul B. Tomascak and an anonymous reviewer and editorial handling by Richard Carlson. We also like to thank Soodabeh Durali-Müller for technical support in the chemistry laboratory (University of Frankfurt). This research used samples provided by the Ocean Drilling Program (ODP). ODP is sponsored by the U.S. National Science Foundation (NSF) and participating countries under management of Joint Oceanographic Institutions (JOI), Inc. This study was supported by the Swiss National Science Foundation Grant 200020-112149.

Appendix A. Model parameters used for Fig. 5

For $\delta^{11}B$, we use a combined fractionation factor (as for Fig. 4), considering the equilibrium fractionation between $B(OH)_3$ and $B(OH)_4^-$ in a fluid and the fractionation between $B(OH)_4^-$ (aq) and silicates (Liu and Tossell, 2005, and reported in Supplementary Table 2). For B and Li it is assumed that no further isotope fractionation takes place when the adsorbed species are integrated into the mineral lattice (Palmer and Swihart, 1996). For B, we calculate the $\delta^{11}B$ evolution in fluid and rock as a function of temperature at constant pH (8.2; Fig. 5A) and as a function of pH at constant temperature (200 °C; Fig. 5B). For Li, we use a minimum fractionation of −4‰ (Chan et al., 1992), which was established for weathering of basalt on the ocean floor. Further on, we apply a maximum fractionation of −21‰ (Vigier et al., 2008), assuming the Li isotope fractionation between seawater and serpentine is similar to that between seawater and missing phase in the ocean.

For B, the fluid evolution model is based on the assumption of equilibrium between the two dissolved B isotopes (^{10}B and ^{11}B) in the fluid. As B is removed from the solution by reaction with the rock, the tetrahedral form is preferentially adsorbed on the mineral surface and later integrated into the lattice, according to the fractionation between $B(OH)_4$ (aq) and BO_4 in silicates (Liu and Tossell, 2005). If no isotopic fractionation between $B(OH)_4$ and BO_4 occurs, the adsorbed B has the same isotopic signature as the dissolved tetrahedral species. As re-equilibration between dissolved and adsorbed B occurs, the isotopic ratio of the total adsorbed B is at any time equal to that of the dissolved tetrahedral species plus the mineral fractionation. With proceeding fluid–rock interaction, the fraction of ^{11}B in the fluid increases as ^{10}B prefers tetrahedral coordination. A rock reacting with an evolved fluid that has already lost large parts of its B will thus have much heavier $\delta^{11}B$ than a rock reacting with virtually unchanged seawater.

Li in aqueous solutions is highly hydrated and usually assumes tetrahedral coordination (Olsher, 1991). It was shown that during low-temperature weathering of soils, surface water preferentially removes ^7Li (Pistiner and Henderson, 2003). Seafloor weathering leads to a fractionation $\Delta^7Li_{seawater-rock}$ of −4‰ (Chan et al., 1992; Chan et al., 1993). As shown by Vils et al. (2008), Li is leached during serpentinization at ODP Leg 209, thus the δ^7Li of the coexisting fluid becomes lighter (Fig. 5C).

Appendix B. Supplementary data

Supplementary data associated with this article can be found, in the online version, at doi:10.1016/j.epsl.2009.07.005.

References

Albarède, F., Michard, A., Minister, J.F., Michard, G., 1981. $^{87}Sr/^{86}Sr$ ratio in hydrothermal water and deposits from the East Pacific Rise at 21°N. Earth Planet. Sci. Lett. 55, 229–236.

Alt, J.C., Shanks III, W.C., Bach, W., Paulick, H., Garrido, C.J., Beaudoin, G., 2007. Hydrothermal alteration and microbial sulfate reduction in peridotite and gabbro exposed by detachment faulting at the Mid-Atlantic ridge, 15°20′N (ODP Leg 209): a sulfur and oxygene isotope study. Geochem. Geophys. Geosystems 8, 1–22.

Bach, W., Garrido, C.J., Paulick, H., Harvey, J., Rosner, M., 2004. Seawater–peridotite interactions: first insights from ODP Leg 209, MAR 15°N. Geochem. Geophys. Geosystems 5, 1–22.

Barnes, J.D., Paulick, H., Sharp, Z.D., Bach, W., Beaudoin, G., 2009. Stable isotopes ($\delta^{18}O$, δD, $\delta^{37}Cl$) evidence for multiple fluid histories in mid-Atlantic abyssal peridotites (ODP Leg 209). Lithos 110, 83–94.

Barnes, J.D., Sharp, Z.D., 2006. A chlorine isotope study of DSDP/ODP serpentinized ultramafic rocks: insights into the serpentinization process. Chem. Geol. 228, 246–265.

Benton, L.D., Ryan, J.G., Savov, I.P., 2004. Lithium abundance and isotopic systematics of forearc serpentinites, Conical Seamount, Mariana forearc: insights into the mechanics of slab-mantle exchange during subduction. Geochem. Geophys. Geosystems 5, 1–14.

Benton, L.D., Ryan, J.G., Tera, F., 2001. Boron isotope systematics of slab fluids as inferred from a serpentine seamount, Mariana forearc. Earth Planet. Sci. Lett. 187, 273–282.

Bonatti, E., Lawrence, J., Morandi, N., 1984. Serpentinization of oceanic peridotites: temperature dependence of mineralogy and boron content. Earth Planet. Sci. Lett. 70, 88–94.

Boschi, C., 2006. Building Lost City: Serpentinization, mass transfer and fluid flow in an oceanic core complex. PhD-thesis ETH Zürich.

Boschi, C., Dini, A., Früh-Green, G., Kelley, D.S., 2008. Isotopic and element exchange during serpentinization and metasomatism at the Atlantis Massif (MAR 30°N): insights from B and Sr isotope data. Geochim. Cosmochim. Acta 72, 1801–1823.

Bouman, C., Elliott, T., Vroon, P.Z., 2004. Lithium inputs to subduction zones. Chem. Geol. 212, 59–79.

Brooker, R.A., James, R.H., Blundy, J.D., 2004. Trace elements and Li isotope systematics in Zabargad peridotites: evidence of ancient subduction processes in the Red Sea mantle. Chem. Geol. 212, 179–204.

Cannat, M., 1993. Emplacement of mantle rocks in the seafloor at mid-ocean ridges. J. Geophys. Res. 98, 4163–4172.

Catanzaro, E.J., Champion, C.E., Garner, E.L.G.M., Sappenfield, K.M., Shields, K.M., 1970. Boric acid: isotopic and assay standard reference materials. US Nat. Bur. Standards Spec. Publ., vol. 260–17. 70pp.

Chan, L.H., Alt, J.C., Teagle, D.A.H., 2002. Lithium and lithium isotope profiles through the upper oceanic crust: a study of seawater-basalt exchange at ODP Sites 504B and 896A. Earth Planet. Sci. Lett. 201, 187–201.

Chan, L.H., Edmond, J., 1988. Variation of lithium isotope composition in the marine environment: a preliminary report. Geochim. Cosmochim. Acta 52, 1711–1717.

Chan, L.H., Edmond, J., Thompson, G., 1993. A lithium isotope study of hot springs and metabasalts from Mid-Ocean ridge hydrothermal systems. J. Geophys. Res. 98, 9653–9659.

Chan, L.H., Edmond, J., Thompson, G., Gillis, K.M., 1992. Lithium isotopic composition of submarine basalts: implications for the lithium cycle in the oceans. Earth Planet. Sci. Lett. 108, 151–160.

Davies, A.C., Bickel, M.J., Teagle, D.A.H., 2003. Imbalance in the oceanic strontium budget. Earth Planet. Sci. Lett. 211, 173–187.

Decitre, S., Deloule, E., Reisberg, L., James, R., Agrinier, P., Mével, C., 2002. Behavior of Li and its isotopes during serpentinization of oceanic peridotites. Geochem. Geophys. Geosystems 3.

Delacour, A., Früh-Green, G., Frank, M., Gutjahr, M., Kelley, D.S., 2008. Sr- and Nd-isotope geochemistry of the Atlantis Massif (30°N, MAR): implications for fluid fluxes and lithospheric heterogeneity. Geochim. Cosmochim. Acta 254, 19–35.

Douville, E., Charlou, J.L., Oelkers, E.H., Bienvenu, P., Jove Colon, C.F., Donval, J.P., Fouquet, Y., Prieur, D., Appriou, P., 2002. The rainbow vent fluids (36°14′N, MAR): the influence of ultramafic rocks and phase separation on trace metal content in mid-Atlantic ridge hydrothermal fluids. Chem. Geol. 184, 37–48.

Edmond, J., Measures, C., McDuff, R.E., Chan, L.H., Collier, R., Grant, B., Gordon, L.I., Corliss, J.B., 1979. Ridge crest hydrothermal activity and the balance of the major and minor elements in the ocean: the Galapagos data. Earth Planet. Sci. Lett. 46, 1–18.

Elliott, T., Jeffcoate, A., Bouman, C., 2004. The terrestrial Li isotope cycle: light-weight constraints on mantle convection. Earth Planet. Sci. Lett. 220, 231–245.

Escartin, J., Mével, C., MacLeod, C.J., McCaig, A.M., 2003. Constraints on deformation conditions and the origin of oceanic detachments: the mid-Atlantic ridge core complex at 15°45′N. Geochem. Geophys. Geosystems 4, 1–37.

Flesch, G., Anderson, A.R., Svec, H.J., 1973. A secondary isotopic standard for $^6Li/^7Li$ determinations. Int. J. Mass Spectrom. Ion Phys. 12, 265–272.

Foustoukos, D.I., James, R.H., Berndt, M.E., Seyfried, W.E., 2004. Lithium isotopic systematics of hydrothermal vent fluids at the Main Endeavour Field, Northern Juan de Fuca Ridge. Chem. Geol. 212, 17–26.

Foustoukos, D.I., Savov, I.P., Janecky, D.R., 2008. Chemical and isotopic constraints on water/rock interactions at the Lost City hydrothermal field, 30°N Mid-Atlantic ridge. Geochim. Cosmochim. Acta 72, 5457–5474.

Frost, B.R., Beard, J.S., 2007. On silica activity and serpentinization. J. Petrol. 48, 1351–1368.

Godard, M., Lagabrielle, Y., Alard, O., Harvey, J., 2008. Geochemistry of the highly depleted peridotites drilled at ODP Sites 1272 and 1274 (Fifteen–Twenty Fracture Zone, Mid-Atlantic Ridge): implications for mantle dynamics beneath a slow spreading ridge. Earth Planet. Sci. Lett. 267, 410–425.

Hart, S.R., Blusztajn, J., Dick, H.J.B., Meyer, P.S., Muehlenbachs, K., 1999. The fingerprint of seawater circulation in a 500-meter section of ocean crust gabbros. Geochim. Cosmochim. Acta 63, 4059–4080.

Hemming, N.G., Reeder, R.J., HG, N., 1995. Mineral-fluid partitioning and isotopic fractionation of boron in synthetic calcium carbonate. Geochim. Cosmochim. Acta 59, 371–379.

Huh, Y., Chan, L.H., Zhang, L., Edmond, J., 1998. Lithium and its isotopes in major world rivers: implications for weathering and the oceanic budget. Geochim. Cosmochim. Acta 62, 2039–2051.

Ishikawa, A., Nakamura, E., 1992. Boron isotope geochemistry of the oceanic crust from DSDP/ODP Hole 504B. Geochim. Cosmochim. Acta 56, 1633–1639.

Ishikawa, T., Nakamura, E., 1993. Boron isotope systematics of marine sediments. Earth Planet. Sci. Lett. 117, 567–580.

Kakihana, H., Kotaka, M., 1977. Equilibrium constants for boron isotope-exchange reactions. Bull. Res. Lab. Nucl. React 2, 1–12.

Kasemann, S., Meixer, A., Rocholl, A., Vennemann, T., Rosner, M., Schmitt, A.K., Wiedenbeck, M., 2001. Boron and Oxygen isotopic composition of certified reference materials NIST SRM 610/612 and reference materials JB-2 and JR-2. Geostand. Newsl. 25, 405–416.

Kelemen, P.B., Kikawa, E., Miller, D.J., 2004. Proceedings of the Ocean Drilling Program. Preliminary Report Leg, vol. 209.

Kelemen, P.B., Kikawa, E., Miller, D.J., 2007. Proc. ODP, Sci. Results, vol. 209. Ocean Drilling Program, College Station, TX.

Kelley, D.S., Karson, J.A., Blackman, D.K., Früh–Green, G., Butterfield, D.A., Lilley, M.D., Olson, E.J., Schrenk, M.O., Roe, K., Lebon, G.T., Rivizzigno, P., 2001. An off-axis hydrothermal field near the mid-Atlantic ridge at 30°N. Nature 412, 145–149.

Li, Y.H., 1982. A brief discussion on the mean oceanic residence time of elements. Geochim. Cosmochim. Acta 46, 2671–2675.

Liu, Y., Tossell, A., 2005. Ab initio molecular orbital calculations for boron isotope fractionations on boric acids and borates. Geochim. Cosmochim. Acta 69, 3995–4006.

MacDonald, A.H., Fyfe, W.S., 1985. Rate of serpentinization in seafloor environments. Tectonophysics 116, 123–135.
McCaig, A.M., Cliff, R.A., Escartin, J., Fallick, A.E., MacLeod, C.J., 2007. Oceanic detachment faults focus very large volumes of black smoker fluids. Geology 35, 935–938.
McCulloch, M., Gregory, R.T., Wasserburg, G.J., Taylor, H.P.J., 1980. A neodymium, strontium and oxygen isotopic study of the cretaceous Semail ophiolite and implications for the petrogenesis and seawater-hydrothermal alteration of oceanic crust. Earth Planet. Sci. Lett. 46, 201–211.
Mével, C., 2003. Serpentinization of abyssal peridotites at mid-ocean ridges. Compte Rendus Geosc. 335, 825–852.
Michael, P.J., Langmuir, C.H., Dick, H.J.B., Snow, J.E., Goldstein, S.L., Graham, D.W., Lehnert, K., Kurras, G., Jokat, W., Mühe, R., Edmonds, H.N., 2003. Magmatic and amagmatic seafloor generation at the ultraslow-spreading Gakkel ridge, Arctic Ocean. Nature 423, 956–961.
Millot, R., Guerrot, C., Vigier, N., 2004. Accurate and high-precision measurement of lithium isotopes in two reference materials by MC-ICP-MS. Geostand. Geoanal. Res. 28, 153–159.
Nakamura, E., Ishikawa, T., Birk, J.L., Allègre, C.J., 1992. Precise boron analysis of natural rock samples using a boron mannitol complex. Chem. Geol. 94, 193–204.
Niu, Y., 2004. Bulk-rock major and trace element compositions of abyssal peridotites: implications for mantle melting, melt extraction and post-melting processes beneath mid-ocean ridges. J. Petrol. 45, 2423–2458.
Olsher, U., 1991. Coordination chemistry of lithium ion: a crystal molecular structure. Chem. Rev. 91, 137–164.
Palmer, M.R., 1991. Boron isotope systematics of hydrothermal fluids and tourmalines: a synthesis. Chem. Geol. 94, 111–121.
Palmer, M.R., Edmond, J., 1989. The strontium isotope budget of the modern ocean. Earth Planet. Sci. Lett. 92, 11–26.
Palmer, M.R., Spivack, A.J., Edmond, J., 1987. Temperature and pH controls over isotopic fractionation during adsorption of boron on marine clay. Geochim. Cosmochim. Acta 51, 2319–2323.
Palmer, M.R., Swihart, G.H., 1996. Boron Isotope Geochemistry: An Overview, vol. 33. Mineralogical Society of America, Washington, D.C., pp. 709–740.
Paulick, H., Bach, W., Godard, M., De Hoog, J.C.M., Suhr, G., Harvey, J., 2006. Geochemistry of abyssal peridotites (mid-Atlantic ridges, 15°20′N, ODP Leg 209): implications for fluid/rock interaction in slow spreading environments. Chem. Geol. 234, 179–210.
Pelletier, L., 2008. The oceanic mantle as an important repository for the light elements Li, Be and B. PhD-Thesis. University of Neuchâtel.
Pelletier, L., Vils, F., Kalt, A., Gméling, K., 2008. Li, B and Be contents of harzburgites from the Dramala Complex (Pindos ophiolite, Greece): evidence for a MOR-type mantle in a supra-subduction zone environment. J. Petrol. 49, 2043–2080.
Pennisi, M., Leeman, W.P., Tonarini, S., Pennisi, A., Nabelek, P.I., 2000. Boron, Sr, O and H isotope geochemistry of groundwaters from Mt. Etna (Sicily) — hydrologic implications. Geochim. Cosmochim. Acta 64, 961–974.
Pistiner, J.S., Henderson, G.M., 2003. Lithium-isotope fractionation during continental weathering processes. Earth Planet. Sci. Lett. 214, 327–339.
Pokrovsky, O.S., Schott, J., Castillo, A., 2005. Kinetics of brucite dissolution at 25 °C in the presence of organic and inorganic ligands and divalent metals. Geochim. Cosmochim. Acta 69, 905–918.
Quinby-Hunt, M.S., Turekian, K.K., 1983. Distribution of elements in seawater. EOS 64, 130–132.
Ranero, C.R., Morgan, P.J., McIntosh, K., Reichert, C., 2003. Bending-related faulting and mantle serpentinization at the Middle America trench. Nature 45, 367–373.
Rehkamper, M., Hofmann, A.W., 1997. Recycled ocean crust and sediment in Indian Ocean MORB. Earth Planet. Sci. Lett. 147, 93–106.
Ryan, J.G., Langmuir, C.H., 1987. The systematics of lithium abundances in young volcanic rock. Geochim. Cosmochim. Acta 51, 1727–1741.
Ryan, J.G., Langmuir, C.H., 1993. The systematics of boron abundances in young volcanic rocks. Geochim. Cosmochim. Acta 57, 1489–1498.
Sakai, R., Kusakabe, M., Noto, M., Ishii, T., 1990. Origin of waters responsible for serpentinization of the Izu–Ogasawara–Mariana forearc seamounts in view of hydrogen and oxygen isotope ratios. Earth Planet. Sci. Lett. 100, 291–303.
Salters, V.J.M., Stracke, A., 2004. Composition of the depleted mantle. Geochem. Geophys. Geosystems 5, 1–27.
Savov, I.P., Ryan, J.G., D'Antonio, M., Fryer, P., 2007. Shallow slab fluid release across and along the Mariana arc-basin system: insights from geochemistry of serpentinized peridotites from the Mariana Forearc. J. Geophys. Res. 112.
Savov, I.P., Ryan, J.G., D'Antonio, M., Kelley, K., Mattie, P., 2005. Geochemistry of serpentinized peridotites from the Mariana Forearc Conical Seamount, ODP Leg 125: implications for the elemental recycling at subduction zones. Geochem. Geophys. Geosystems 6, 1–24.
Schmidt, K., Koschinsky, A., Garbe-Schönberg, D., de Carvalho, L.M., Seifert, R., 2007. Geochemistry of hydrothermal fluids from the ultramafic-hosted Logatchev hydrothermal field, 15°N on the mid-Atlantic ridge: temporal and spatial investigation. Chem. Geol. 242, 1–21.
Seitz, H.M., Brey, G.P., Lahaye, Y., Durali, S., Weyer, S., 2004. Lithium isotopic signatures of peridotite xenoliths and isotopic fraction at high temperature between olivine and pyroxenes. Chem. Geol. 212, 163–177.
Sen, S., Stebbins, J.F., Hemming, N.G., Ghosh, B., 1994. Coordination environments of B impurities in calcite and aragonite polymorphs: a ^{11}B MAS NMR study. Am. Mineral. 79, 819–825.
Seyfried, W.E., Chen, X., Chan, L.H., 1998. Trace element mobility and lithium isotope exchange during hydrothermal alteration of seafloor weathered basalt: an experimental study at 350 °C, 500 bars. Geochim. Cosmochim. Acta 62, 949–960.
Seyfried, W.E., Janecky, D.R., Mottl, M.J., 1984. Alteration of the oceanic crust: implications for geochemical cycles of lithium and boron. Geochim. Cosmochim. Acta 48, 557–569.
Seyfried, W.E., Dibble, W.E., 1980. Seawater–peridotite interaction at 300 °C and 500 bars: implications of the origin of oceanic serpentinites. Geochim. Cosmochim. Acta 44, 309–321.
Seyler, M., Lorand, J.P., Dick, H.J.B., Drouin, M., 2007. Pervasive melt percolation reactions in ultra-depleted refractory harzburgites at the mid-Atlantic ridge, 15°20′N: ODP Hole 1274A. Contrib. Mineral. Petrol. 153, 303–319.
Simon, L., Lécuyer, C., Maréchal, C., Coltice, N., 2006. Modelling the geochemical cycle of boron: implications for the long-term δ^{11}B evolution of seawater and oceanic crust. Chem. Geol. 225, 61–76.
Smith, H.J., Spivack, A.J., Staudigel, H., Hart, S.R., 1995. The boron isotopic composition of altered oceanic crust. Chem. Geol. 126, 119–135.
Spivack, A.J., Edmond, J., 1987. Boron isotope exchange between seawater and oceanic crust. Geochim. Cosmochim. Acta 51, 1033–1043.
Spooner, E.T.C., Chapman, H.J., Smewing, J.D., 1977. Strontium isotopic contamination and oxidation during ocean floor hydrothermal metamorphism of the ophiolitic rocks of the Troodos Massif, Cyprus. Geochim. Cosmochim. Acta 41, 873–890.
Stein, C.A., Stein, S., 1992. A model for the global variations in oceanic depth and heat flow with lithospheric age. Nature 359, 123–129.
Stein, S., Stein, C.A., 1996. Thermo-mechanical evolution of oceanic lithosphere: Implications for the subduction process and deep earthquakes (overview). In: Bebout, GE, Scholl, DW, Kirby, SH, Platt, JP (Eds.), Subduction: Top to Bottom, vol. 96, pp. 1–17.
Suhr, G., Kelemen, P.B., Paulick, H., 2008. Microstructures in Hole 1274A peridotites, ODP Leg 209, mid-Atlantic ridge: tracking the fate of melts percolation in periodotite as the lithosphere is intercepted. Geochem. Geophys. Geosystems 9, 1–23.
Taylor, H.P.J., 1977. Water/rock interactions and the origin of H_2O in granitic batholiths. J. Geol. Soc. (Lond.) 133, 509–558.
Thompson, G., Melson, W.G., 1970. Boron contents of serpentinites and metabasalts in the oceanic crust: implications for the boron cycle in the oceans. Earth Planet. Sci. Lett. 8, 61–65.
Tomascak, P.B., 2004. Developments in the understandings and application of lithium isotopes in earth and planetary sciences. Rev. Mineral. Geochem. 55, 153–195.
Tomascak, P.B., Langmuir, C.H., Le Roux, P.J., Shirley, S.B., 2008. Lithium isotopes in global mid-ocean ridge basalts. Geochim. Cosmochim. Acta 72, 1626–1637.
Tonarini, S., Pennisi, M., Adomi-Braccesi, A., Dini, A., Ferrara, G., Gonflantini, R., Wiedenbeck, M., Gröning, M., 2003. Intercomparison of boron isotope and concentration measurements. Part I: selection, preparation and homogeneity tests of the intercomparison material. Geostand. Newsl. 27, 21–39.
Vigier, N., Decarreau, A., Millot, R., Carignan, J., Petit, S., France-Lanord, C., 2008. Quantifying Li isotope fractionation during smectite formation and implications for the Li cycle. Geochim. Cosmochim. Acta 72, 780–792.
Vils, F., Pelletier, L., Kalt, A., Müntener, O., Ludwig, T., 2008. The lithium, boron and beryllium content of serpentinized peridotites from ODP Leg 209 (Sites 1272A and 1274A): implications for lithium and boron budgets of oceanic lithosphere. Geochim. Cosmochim. Acta 72, 5475–5504.
Wei, W., Kastner, M., Dehyle, A., Spivack, A.J., 2005. Geochemical cycling of fluorine, chlorine, bromine, boron and implications for fluid–rock reactions in Mariana forearc, South Chamorro Seamount, ODP Leg 195. Proceedings of Ocean Drilling Program, Scientific Results, vol. 195, pp. 1–23.
Wunder, B., Meixner, A., Romer, R.L., Heinrich, W., 2006. Temperature-dependent isotopic fractionation of lithium between clinopyroxene and high-pressure hydrous fluids. Contrib. Mineral. Petrol. 151, 112–120.
You, C.F., Spivack, A.J., Grieskes, J.M., Rosenbauer, R., Bischoff, J.L., 1995. Experimental study of boron geochemistry: implications for fluid processes in subduction zones. Geochim. Cosmochim. Acta 59, 2435–2442.
Zhang, L., Chan, L.H., Gieskes, J.M., 1998. Lithium isotope geochemistry of pore waters from Ocean Drilling Program Sites 918 and 919, Irminger Basin. Geochim. Cosmochim. Acta 62, 2437–2450.